Design and development of essential oil based nanoemulsion for topical application of triclosan for effective skin antisepsis.

Pratibha G. Kakadia[a] & Barbara R. Conway[a,b*]

[a]*Department of Pharmacy, School of Applied Sciences, University of Huddersfield, Huddersfield, UK*

[b]*Institute of Skin Integrity and Infection Prevention, University of Huddersfield, Huddersfield, UK*

*Corresponding author
pratibha@ibhri.org

Abstract

The skin acts as physical barrier to protect the body from external physical and chemical environment. When skin is infected, the outer epidermal barrier is compromised and colonized with microbial growth. Wound infection presents an immense burden in healthcare costs and decreased quality of life for patients. Topical application of nanoemulsions (NE) at pathological sites offers the potential advantage of direct drug delivery to the skin including potential for follicular targeting. This may have application in the improvement of skin antisepsis. In this study, NEs of triclosan (TSN) were prepared using hot high shear homogenization followed by ultrasonication. The oil phases comprised eucalyptus oil (EO) and olive oil (OO) and pseudo-ternary phase diagrams used to select optimum concentrations of surfactant. EO-based NEs had smaller droplet size and higher entrapment efficiency compared to OO-based NEs. Skin permeation was higher for EO-containing formulations, likely due to higher solubility of TSN in EO, smaller droplet size, low viscosity, and permeation enhancement effects of EO. Significantly, TSN was retained within the skin, demonstrating the potential of NEs for targeting hair follicular delivery within the skin, which may help improve the success of topical antisepsis.

Keywords: Triclosan, nanoemulsion, eucalyptus oil, olive oil, hair follicular drug delivery, wound healing.

Abbreviations:
Nanoemulsions:NEs; triclosan :TSN; eucalyptus oil :EO; olive oil:OO; Transmission electron microscopy:TEM; Tween 80:T80; Span 80:S80; High shear homogenization:HSH

1. Introduction

The cutaneous microbiota comprises a diverse range of bacteria, fungi and viruses. These may be altered in some disease conditions and when the skin barrier is broken, as in wound formation. The goal of wound management is to provide the most favourable environment for regeneration of damaged epidermis, while protecting the site from trauma and infection. An open wound is at risk of microbial infections; the majority of infected wounds present polymicrobial and are often contaminated by the microflora available within the adjacent skin and mucous membranes.

The increasing use of antibiotics is leading to issues with antimicrobial resistance and the topical use of antiseptics for wound care can play an important role in antimicrobial stewardship strategies, reducing the need for antibiotic prescribing in prophylaxis and treatment. There is a wide spectrum of non-antibiotic antimicrobial agents used in managing wounds, with many antiseptic solutions used for skin cleansing and decontaminating sites colonised by antibiotic resistance strains. The activity of most non-antibiotic antimicrobial agents is influenced by their concentration, formulation, and contact time (Cooper and Kirketerp 2018; Maillard 2013).

There is a resident bacterial population on the skin throughout the body. These colonizing bacteria are divided into resident, transient and infectious flora. While resident bacteria are present without causing any infections to skin, a transient bacterial population can cause severe skin infections. The localization of bacteria within the epidermis and skin appendages can act as potential microbial reservoirs (Lange-Asschenfeldt et al. 2011) with 25% of the resident bacterial flora in the skin residing within hair follicles, hence, there is a need to develop topical non-toxic antimicrobial formulations which can penetrate and remain in the epidermis and target drug delivery to hair follicles to treat and prevent skin infections.

Nanoemulsions (NEs), with their small droplet size, ease of manufacture and high drug-loading capacity, are one of the most promising approaches for enhancing the skin permeability of an active substance. The efficiency by which a surfactant stabilises the oil-water interface is an important consideration in their manufacture. During the high-energy processes often required to produce the nanoemulsion, it is important to ensure that enough surfactant is rapidly adsorbed to the newly formed droplet surface and covers it well enough to prevent coalescence. With respect to the active ingredient in a formulation, the primary goal in using NEs as a carrier system is to protect and deliver the active ingredient. Hence, the compatibility of formulation ingredients with the active ingredient and the capacity of formulation ingredients to solubilise and stabilise the active ingredient must be considered. Prerequisite information, such as the physicochemical properties of the active ingredient, is needed to select an appropriate surfactant system and oil phase.

In the present study, we have prepared NEs containing triclosan (TSN), eucalyptus oil (EO) and olive oil (OO) which have antibacterial and antifungal properties (Sugumar et al. 2014; Ghiasia et al. 2019). NEs were prepared containing EO and OO in different concentrations, along with the use of Tween 80 (T80) and Span 80 (S80) as a surfactant and cosurfactant mixture (S_{mix}) respectively. The developed NE formulations were compared with a control solution (a saturated aqueous solution of TSN) for stability, physicochemical characterisation, and skin permeation, including follicular targeting.

It is very difficult to predict *in vivo* distribution of topically applied solutes within skin based on *in vitro* experiments. Hence, *in vitro* skin permeation has been modelled according to Anissimov and Roberts (2011) to explore and understand the dermal deposition. The study was based on a pharmacokinetic model describing the effect of

blood flow, blood protein binding and dermal binding on the rate and depth of penetration of topical drugs into the underlying skin. This interpretation can be used to understand *in vitro* dermal penetration studies.

2. Materials and methods

2.1 Materials

Triclosan powder was gifted by Vivimed Labs Ltd, (India). Eucalyptus oil, olive oil, Tween 80, Span 80, sodium lauryl sulphate were purchased from Sigma Aldrich (UK). All other reagents were of analytical grade.

2.2 Chromatographic detection of triclosan

Chromatographic analysis of TSN was performed on a Shimadzu HPLC equipped with a SPD-20 AV Prominence UV/visible detector set at 280 nm, an LC- 20AT pump, and SIL-20A Prominence autosampler. Separation of TSN was performed using a KinetexVR pentaflurophenyl 5 µm column (250 4.6 mm) (Phenomenex, Macclesfield, UK) maintained at 30 °C and TSN was eluted with a mobile phase consisting of acetonitrile and water (60:40 v/v) at a flow rate of 1 ml/min. Injection volume was 5 µl with retention time of 7.34 min (Kakadia and Conway 2018).

2.3 Determination of the solubility of triclosan in oils and surfactants.

The solubility of TSN in the different components of NE was carried out by adding excess TSN to aliquots of EO, OO, T80, S80 and control [PBS (pH 7.4) containing 1% SLS (150mM)] in stoppered vials of 5 ml and mixed using a vortex mixer. The vials were then kept at 25±1.0°C in an isothermal shaker for 72 h to reach equilibrium. The equilibrated samples were removed from the shaker and centrifuged at 4,000 rpm ((Eppendorf AG 5702, Germany) for 15 min. The supernatant was filtered through a 0.22-µm membrane filter. The supernatant was mixed with equal volume of mobile phase to determine the concentration of TSN using HPLC.

2.4 Construction of pseudo-ternary phase diagrams

Phase diagrams of surfactants, co-surfactants, oil and water phases were plotted by mixing pre-weighed ingredients, titrating with water and stirred well at room temperature. Hydrophilic lipophilic balance (HLB) of S_{mix} was calculated using molar ratios; HLB of T80 is 15 and S80 is 4.3 (Kaseem et al. 2019). For each phase diagram, different combinations of oils and S_{mix} were used in different volume ratios from 1:9 to 9:1 (Lawrence et al. 2000). Monophasic/biphasic systems were confirmed visually; where turbidity appeared, the formulation was considered biphasic but once clear and transparent mixture are visualized after stirring the formulation is considered as end point and at this point water titration was stopped. These were marked in the phase diagram and the area covered by these points was identified as the NE region of the formulation.

2.5 Preparation of nanoemulsion

TSN-NEs were prepared using a previously described high speed homogenisation (HSH) method, followed by ultra-probe sonication (Tripathy 2014). Briefly, the oil phase containing TSN (equivalent to 10 mg/g of formulation) was prepared by heating oils (EO and OO) to 40ºC to increase drug loading into the formulation. Based on the solubility data (Table 2), formulation needed double amount of TSN loading compare to its solubility at 25ºC. The hot oil phase was added slowly to the hot aqueous phase containing Smix and water under HSH (Silverson, Chesham, UK). This hot primary emulsion was then subjected to probe ultrasonication (Sonics and Materials Inc., Newtown, CT) for 15 min at 70% frequency amplitude. The evaluated NE systems and their compositions are summarized in Table 1.

2.6 Measurement of NEs droplet size and zeta potential.

The mean droplet size and polydispersity index (PDI) of the NEs were determined by

Zetasizer Nano ZS (Malvern Instruments Ltd, Malvern, UK) and followed by zeta potential measurement. For droplet size measurements, samples were diluted at 1:100 in water and measured in triplicate with 15 runs each at 25 ◦C in backscattering mode. The zeta potential was determined in triplicate by diluting each sample 1:10 in water at 25 ◦C with 10 to 50 runs per measurement (Chou et al. 2021, Demisli et al. 2020).

2.7 Determination of viscosity and pH

The viscosities of the NE formulations were evaluated using Bohlin Gemini cone and plate rheometer (Aimil Ltd., India) at 25 °C in triplicate. The pH of the NE formulations was measured at ambient temperature using a digital pH meter. Each pH value was measured in triplicate and average value (mean ± SD) was recorded.

2.8 Encapsulation efficiency

The percent encapsulation efficiency (%EE), which corresponds to the percentage of TSN encapsulated within the NEs, was determined by measuring the concentration of free TSN as well as the total concentration of TSN in the dispersion medium (Prasad et al. 2020). Most literature studied (Chou et al. 2021, Sarheed et al. 2019) the % EE of developed NE using similar method.

To measure total TSN concentration 1 mL of NE was dissolved in a chloroform and methanol (1:1) mixture and centrifuged at 4000 rpm for 20 min and the obtained supernatant was analysed using HPLC. The analysis was performed in triplicate and % EE was calculated using following equation 1.

$$\text{EE (\%)} = \frac{Total\ amount\ of\ drug\ added - Amount\ of\ drug\ in\ the\ supernatant\ x\ 100}{Total\ amount\ of\ drug\ added} \qquad (1)$$

2.9 Transmission electron microscopy

The morphology of NEs was confirmed using transmission electron microscopy (TEM- JEOL 3010). The NEs was diluted with water and a drop was placed on a 20-mesh carbon coated copper grid (Agar Scientific, Stansted, UK). Excess sample was removed with filter paper and the samples were negatively stained with 1% (w/w) phosphotungstic acid for 1 min, air dried at room temperature and images were recorded using Megaview camera at 300 kV.

2.10 Thermodynamic stability study

The NE formulations were subjected to temperature stress studies carried out in three stages: centrifugation, heating -cooling and freeze-thawing for 3 cycles over 6 days (Loo et al. 2011; Srilatha et al. 2013)

Centrifugation stage: All the samples were centrifuged at 4400 rpm for 20 min (Eppendorf AG5702, Germany). The formulations were inspected visually for any phase separation, sedimentation and creaming.

Heating-cooling stage: The effect of change in temperature on the stability of NEs was analysed by storing the samples between 4°C and 40°C for a period of 48 h. All the formulations were examined for any physical instability and only stable formulations were subjected to freeze thaw cycling.

Freeze-thaw cycling stage: The formulations were subjected to -20°C and 25°C for a period of 48 h each. Freeze-thaw cycles were performed in triplicate and samples were visually examined for phase separation.

All formulation which found to be stable after all three temperature stress studies were subjected to further characterization studies.

2.11 In vitro skin permeation study

The skin permeation of TSN (n=6 for each formulation and control) was assessed over a period of 24 h using vertical Franz diffusion cells with a diffusion area of 3.8 cm^2

and a receiver compartment volume of 30 mL. Frozen excised full-thickness porcine ear skin was thawed for 30 min and then hydrated by immersing in phosphate buffer saline (PBS) pH 7.4 for 60 min prior to the start of each experiment. The receiver compartment contained PBS solution (pH 7.4) with 1% w/w sodium lauryl sulphate (SLS) (150mM), to ensure sink conditions were maintained throughout the study. Water was circulated at 37° C to maintain a skin surface temperature at 32° C, with stirring speed of 200 rpm for 24 h. 1 gm of NE formulation (equivalent of 10 mg TSN) or TSN saturated aqueous solution as a control was applied to the donor compartment (infinite dose). Samples (500 µl) were withdrawn at regular intervals from the receiver compartment and replaced by an equal volume of fresh receiver solution. The amount of TSN permeated through skin over 24 h was analysed by HPLC (Nastiti et al. 2020).

2.12 Quantification of drug from skin

At the end of the permeation study, the amount of TSN retained within the skin was quantified using the adhesive tape stripping method (Yu et al. 2014). After 24 h of diffusion, the skins were carefully removed and washed with distilled water to remove any residual formulation. A differential stripping technique was used to quantify amount of TSN in porcine skin by combining tape stripping and cyanoacrylate biopsy (Teichmann et al. 2005; Wosika and Cal 2010). The skin was tape stripped 15 times using an adhesive surgical tape (3M Transpore, Glasgow, UK). Tape 1 was analysed individually as this would contain unabsorbed materials on the skin surface, whereas tapes 2–5 and 6–15 were analysed together. Following tape stripping, a drop of cyanoacrylate glue was placed on the skin and covered with adhesive tape applied under slight pressure. After 10 min, the cyanoacrylate polymerised and the strip was removed, entrapping the casts of hair follicles. Two successive cyanoacrylate applications were applied to each skin sample and analysed individually. After

stripping, the remaining skin was weighed accurately and cut into fine pieces. All skin samples were placed into vials containing 10 ml of methanol and sonicated for 30 min. After sonication (Transonic, Wisbech, UK), the samples were centrifuged for 20 min at 400 rpm (Eppendorf centrifuge 5702, Camberley, UK). The supernatant was collected after centrifugation and the amount of TSN in remaining skin tissue was determined using HPLC.

2.13 In vitro simulation

Mathematical modelling or simulations of *in vitro* permeation data can provide insight into the underlying mechanisms of skin permeation, which can be useful in translation to *in vivo* (Anissimov and Roberts 2011). Hence simulations of *in vitro* permeation data were performed for eucalyptus oil based NE formulation (EO-6). For simulation studies various parameters were considered and reported in Table 2.

In simulation, the distribution parameter (Kd value) was calculated to provide an indication of the rate-limiting step i.e., distribution of the drug from one compartment to another. In this case Kd value provides an indication of the distribution of NEs formulation from surface of the skin into the dermis of the skin.

(1) Kd Value = $\sqrt{\{\frac{fud \times qb \times Ps}{Dt\ (qb + fub \times Ps)}\}}$

Fud - Fraction of solute unbound in the dermis

Qb - Blood flow rate per unit volume of dermis (0.0014 ml s−1 per ml of dermis) (Cross and Roberts 2006).

Ps - Surface area for skin application

Dt - determined by the dispersion transport with D_{disp} = 5× 10−6 cm2 s−1. Other fitting parameters were A=1 (Anissimov and Roberts 2011).

fub - fraction of solute unbound in the blood (values from *in vitro* permeation study after 24 hours)

(2) Dt = 10.1 × fud (10.1 is the Du , Du is the diffusion rate of unbound solute. with unbound diffusion coefficients being about the same for all solutes), (Anissimov and Roberts 2011; Wilke and Chang 1955).

(3) fud = fub- assumption that unbound fraction can enter the blood circulation because of the pKa of TSN.

2.14 Statistical analysis

Droplet size, ZP and *in vitro* permeation data were compared for statistical significance using a one-way ANOVA, which was performed in triplicate using GraphPad Prism Instat software version 6 (GraphPad, La Jolla, CA, USA) with differences considered to be statistically significant when p values <0.05.

3. Results and Discussion

3.1 Solubility study of triclosan

Solubility of drug is important for formulation design as well as to achieve desirable drug concentration into the formulation system. Therefore, it is necessary to determine the solubility of TSN in different agents, including oil, surfactant, cosurfactant and control solution containing PBS (pH 7.4) with 1% SLS (150mM). EO and OO were selected as oil phase in the formulation. TSN is a poorly water-soluble drug (10 mg/L) and thus it was incorporated into the oil phase of the NEs to formulate it for topical drug delivery (Benita and Levy 1993). Solubility of TSN in selected oils, surfactant, cosurfactant and control are reported in Table 2. The solubility of TSN was found to be highest in EO (5.23 ± 0.02 mg/g) as compared to OO (3.51 ± 0.05 mg/g). This may be attributed to the polarity of the poorly soluble drugs that favours their solubilisation in small/medium molar volume of oils, such as medium-chain triglycerides or mono- or diglycerides (Azeem et al. 2009, Lawrence and Rees 2000).

Among various surfactants, non-ionic ones have advantages, such as reduced toxicity, lower CMC values and higher in vivo stability profiles. Furthermore, they are less affected by changes in pH and ionic strength (Bali et al. 2010). Therefore, a mixture of T80 and S80 was selected as a safe and biocompatible surfactant system that produced a transparent and stable formulation.

The solubility of TSN in control solution was found to be 10.05 ± 0.24 mg/g. This is due to the presence of SLS which forms micelles with hydrophobic molecules. A micelle is a group of surfactant aggregates, which in aqueous solution forms a hydrophilic head with surrounding solvent and hydrophobic tails in the micelle centre. Micelle formation occurs due to presence of SLS above its critical micelle concentration (CMC) i.e. the concentration above which micelles start to form, which is reported as 8.20 mM at 25°C (Aguiar et al. 2003, Elisabet et al. 2005)

3.2 Pseudo-ternary phase diagrams

Phase diagrams were constructed to provide information on nanoemulsion zone and assess relationships between composition variation and nanoemulsion formation. To determine the exact proportion of each component required, and subsequently, attain the best parameters for nanoemulsion formulation, we prepared various TSN-NEs by constructing pseudoternary phase diagrams with water, T80, S80, and EO or OO as the aqueous, surfactant, cosurfactant and oil phases, respectively. Performing the oil titration method for each Smix developed the phase diagrams. The resulting phase diagrams depicting the nanoemulsification region for each combination are presented in Figures 1.

The phase diagrams of EO and OO with T80 and water are displayed in (Figure 1(A)(a),(B)(a)). We observed that when T80 was used alone without cosurfactant

(Smix ratio 1:0), only a small amount of oil phase was incorporated at higher concentrations of T80 for both EO and OO (Figure 1). The maximum amount of oil that could be added was found to be 10% w/w at a high (81% w/w) Smix concentration. When T80 with S80 were used in equal amounts (S_{mix} 1:1; HLB 9.65), a larger NE region was observed, perhaps due to the reduction in interfacial tension and increased fluidity of the interface (Figure 1(A)(b),(B)(b)). As the surfactant concentration was increased to S_{mix} 2:1 (HLB 11.57) and S_{mix} 3:1 (HLB 12.32) (Figure 1(A)(c-d),(B)(c-d)), the NE region increased in size compared to S_{mix} 1:1. It may be due to increasing the surfactant concentration is expected to cause more stability and lead to smaller particle size due to its interfacial activity (Salager, 2002).

When the surfactant concentration was increased in comparison to cosurfactant to S_{mix} 4:1 (HLB 12.82) (Figures 1(A)(e),(B)(e)), the size of the NE region decreased, indicating that the optimum HLB required to balance the oil and water phase system in the NEs had been achieved. These observations suggested that the maximum NE zone was achieved at a Smix ratio of 3:1. Therefore, this ratio was selected for subsequent studies.

3.3 Preparation of nanoemulsions

The types and concentrations of oil and surfactants used in the preparation of TSN-loaded NEs affect the solubility of lipophilic drugs and the physicochemical properties of the formulation, namely its droplet size, density, viscosity, interfacial tension and phase behaviour (Wooster 2008). In the present study, oil-in-water NEs of TSN were prepared using HSH, followed by ultrasonication. The initial batches of EO and OO NEs were prepared using different concentrations of Smix 3:1 (2.5, 5, 7.5 and 10 % w/w), while the concentrations of oil used were 5% and 10% w/w (Table 1). To

minimise droplet collision, a low weight percentage of oil was selected, and excess surfactant was used (up to 10% w/w in order to minimise coalescence).

3.4 Determination of droplet size, zeta potential and percent drug entrapment efficiency

Average droplet size of prepared NEs decreased with increasing homogenization duration for both emulsions. When homogenisation time was increased from 10 min to 20 min, EO-NE droplet size decreased from 293.4 ± 2.93 nm to 87.6 ± 1.21, while OO-NE droplets decreased in size from 321.2 ± 3.25 nm to 96.2 ± 1.72 nm (Figure 2). Similar results were reported by Shahavi et al. (2015) for NEs prepared using a S_{mix} containing T80 and S80 in clove oil. Based on the data obtained, the homogenisation time for the preparation of NEs was set at 20 min.

Zeta potential (ZP) has been identified as an important factor to indicate stability of colloidal systems (Laouini et al. 2012). Negative ZP values were obtained for all the NEs formulation, which ranged between -28.9 ± 1.23 mV and -37.1 ± 1.72 mV (Table 3). This is due to the negatively charged chlorinated poly aromatic phenol groups of TSN. It has been reported that a ZP above |15| mV is required for good colloidal stability, as charged droplets repel one another, thus overcoming the natural tendency to aggregate (Grosse et al. 2002; Tagne et al. 2008). Thus, the obtained ZP values were considered sufficient to prevent droplet coalescence and predict stability of the prepared NEs formulation.

Encapsulation efficiency increased with increasing oil concentrations, for both the EO and OO formulations. The %EEs for EO-2, EO-6, OO-2, and OO-6 were found to be 78.83 ± 1.28, 86.14 ± 0.93, 75.49 ± 1.16, and 81.19 ± 2.15, respectively (Table 3). However, no significant differences ($p>0.05$) in %EE were observed between the EO

and OO NE formulations. The results revealed that the concentration of oil greatly influenced the NE entrapment efficiency.

3.5 Viscosity and pH

The average pH for healthy human skin is between 4 to 6 (Kuo et al. 2020). The pH of dermal formulations is an important factor in avoiding skin irritation or susceptibility to bacterial infection. The pH of all optimised formulations was 5.23 to 5.91 (Table 3), and therefore suitable for topical application.

The shear viscosities of the NEs were measured at a controlled shear rate. Overall, the viscosities of the optimised formulations were low (Table 3), as expected for oil-in-water NEs (Alvarado et al. 2015). EO-2 and OO-2 had low viscosities of 20.08 ± 1.14cp and 22.31 ± 1.29cp, respectively, perhaps due to higher aqueous content. These results were significantly different from ($p < 0.05$) the EO-6 and OO-6 formulations.

It was observed that increased oil concentrations slightly increased the viscosities of the NEs, an effect that could be associated with increased micelle diameter. Similar results have been observed, which concluded that droplet size tends to increase with higher oil content. This phenomenon is usually followed by an increase in the viscosity of systems (Chanamai and McClements 2000; Chiesa et al. 2008; Mayer et al. 2013).

3.7 Morphological study by transmission electron microscopy

A TEM micrograph of a TSN-loaded EO based NE formulation is shown in Figure 3. As can be seen in the displayed image, the observed droplets are spherical in shape, with an average droplet size of 100 nm. The TEM images for all the optimised formulations were similar in size and shape. The droplet size results showed good agreement with the results obtained from droplet size analysis by NTA. Similar morphology was reported by Vatsraj et al. (2014) for clarithromycin OO-NE formulations.

3.8 Thermodynamic stability study

All the prepared formulations were subjected to thermal stability studies that included centrifugation, thermal stress, and freeze-thaw cycles, as described in Section 2.10. The composition of selected NEs and the observations for thermodynamic stability studies are given in Table 4. The results showed that the NE formulations EO-2, EO-6, OO-2, and OO-6 remained stable in all three conditions without considerable changes in physicochemical properties. Phase separation following centrifugation was visible for the rest of the formulations. The NE formulations, which passed the thermodynamic stability screening, were those containing 5 % of S_{mix} and 5 and 10 % of essential oils (EO and OO).

3.9 In vitro skin permeation study

Skin permeation studies were performed to compare the permeation of drug from optimised NE formulations (EO-2, EO-6, OO-2, OO-6) and control (saturated solution of TSN in PBS pH 7.4). Both NE and control has similar TSN concentration in order to keep one element constant to compare the permeation data. The cumulative amounts of TSN that permeated through skin from the NEs and control are shown in Figure 4. The results exhibited almost 3-4 times higher drug permeation from the EO-6 NE formulation compared to control, indicating the suitability of NEs as a carrier for use in dermal delivery of the lipophilic TSN.

Several mechanisms have been proposed to explain the ability of NEs to improve dermal permeation and retention. Solubility of TSN is increased by NE formulation due to presence of a lipophilic oil phase, which favours drug partition into the skin because the fraction of the drug dissolved in the vehicle can enter the skin (Heuschkel et al. 2008). NE formulations interact with lipid layers of SC, enhancing drug permeation and retention into the skin (Malcolmson et al. 1998). Further, it is proposed

that NEs can carry the drug through the skin due to their small droplet size (McClements and Xiao 2012). Thermodynamic activity describes the escaping tendency of the drug from the vehicle into the skin and is the actual driving force for diffusion. The thermodynamic activity of the drug in the formulation is a significant driving force for the release and penetration of the drug into the skin (Hilton et al. 1994). As the drug can be released from the internal phase to the external phase and then from the external phase to the skin, the relative activities may be utilized to monitor the skin permeation rate (Chen et al. 2004, Lee et al. 2003).

The EO-NEs showed 2 times higher drug permeation through the skin compared to the OO-NEs. This might be due to the formulations' physicochemical properties, including higher solubility of TSN in EO, smaller droplet size, lower viscosity and the permeation enhancing the effect of EO. Eucalyptus oil consists of 75 % 1, 8- cineole, a terpene that acts by creating liquid pools in the stratum corneum and disrupting the lipid structure of the stratum corneum, thereby increasing the permeation of drugs in the membrane (Herman and Andrzej 2015; Shen et al. 2015; Moghimipoura et al. 2018). A study by Williams and Barry (1989) reported the penetration enhancement activities of EO through excised human skin using 5-fluorouracil as a model drug. The *in vitro* permeation studies demonstrated that EO-6 (1.38 µg/cm^2) provides greater drug permeation than EO-2 (1.13 µg/cm^2), OO-2 (0.48 µg/cm^2), and OO-6 (0.83 µg/cm^2). The type and concentration of oil affected the flux (Jss) and permeability coefficient of the TSN (Table 5 and Figure 5). The Jss values of EO-6 formulation exhibited 2-fold higher diffusion rate through skin compare to OO-NE formulations and 6-fold higher compare to control ($p<0.002$).

The penetration enhancing effects of essential oils with important biological activities are promising. Lan et al. (2014) determined that essential oils increase the penetration

of hydrophilic drugs as well as lipophilic drugs (such as indomethacin and 5-fluorouracil). They also mentioned that penetration effects of essential oils differ according to the polarity of the drugs. Karpanen et al. (2010), presented that the use of EO, which has antimicrobial activity, in a formulation increases the penetration of chlorhexidine as well as its antimicrobial activity. Similarly in another study adding 25% copaiba oil to the formulation increased both the penetration and anti-inflammatory activity of celecoxib (Quiñones et al. 2018).

A benzalkonium chloride loaded nanoemulsion formulation demonstrated efficacious activity against methicillin-resistant Staphylococcus aureus in vitro in mouse and porcine infected wound models. It promoted wound healing as a consequence of reducing inflammation within deep dermal layers and proinflammatory cytokine levels (Cao et al. 2017). The formulation had previously been shown to reduce both bacterial colonisation and symptoms of inflammation in burn wounds (Hemmila et al. 2010).

These results suggest that NEs can play an important role in enhancing the permeability of drugs through the skin.

3.10 Quantification of triclosan in skin using cyanoacrylate biopsy method

To further determine the amount of TSN penetration into the skin, tape stripping was performed following the methodology in Section 2.12. Figure 5 presents the penetration profiles showing the TSN levels (µg/mg tissue) detected in porcine ear skin after 24 h exposure to various NE formulations. The NE formulations resulted in higher amounts of TSN retained in the skin compared to control (Figure 6), with the difference being statistically significant ($p<0.05$). The small size and large surface area of the NE system enhances the penetration of drug through the skin surface (Nastiti 2020)

The total amount of TSN recovered from tape strips (1-15) for the control solution was 2.15 ± 0.03 µg/mg, compared to the NE formulations, which were 4.89 ± 0.24 µg/mg, 10.35 ± 0.45 µg/mg, 2.91 ± 0.17 µg/mg and 3.51 ± 0.28 µg/mg for EO-2, EO-6, OO-2 and OO-6, respectively. Overall EO based NEs showed more TSN retention within the skin and hair follicles compared to OO based NEs. There is no significant difference between the two EO formulations in terms of retention within the skin. The EO-NEs are retained better within different layers of skin compared to OO-NEs, with the differences being statistically significant ($p<0.05$). This is likely partly due to smaller droplet size, high %EE and lower viscosity of EO based formulations. It also may be due to the permeation enhancement effect of 1,8-cineole and other components of EO (Saporito et al. 2018, Niyaz et al. 2019).

The amount of TSN recovered from skin appendages through cyanoacrylate biopsy was dependent on the concentration of the oil used in the formulations. As concentration of oil increased from 5 to 10 % (w/w) in OO-based NEs, there was 2-fold increase in TSN concentration from 1.02 ± 0.19 µg/mg to 2.02 ± 0.12 µg/mg, while for EO-based NEs, the concentration of TSN increased from 1.35 ± 0.17 µg/mg to 3.79 ± 0.14 µg/mg in the appendages. It was observed that TSN retention in skin was higher for EO-NEs compared to the OO-NEs, which aligns with skin permeation data. Hence, this result suggests that a combination of TSN and EO may be a potential method to improve skin antisepsis in clinical practice. EO contains 1,8-cineole, which has been shown to bind in large quantities to the SC (Cornwell et al. 1996). It is thought to enhance lipophilic drug penetration by increasing the coefficient (partitioning of drug between vehicle and SC), as well as hydrophilic drug penetration by increasing the diffusion coefficient (Cal et al. 2001). It has been also shown that 1,8-cineole partitioning in the skin lipids is heterogeneous, leading to both ordered and

disordered areas in SC lipids (Williams et al. 2006). Furthermore, as is evident from some in vitro assays, 1,8-cineole does not permeate through the skin but tends to be retained within the skin (Cal et al. 2006, Cornwell et al. 1996). Increased skin penetration of steroid hormones using an EO (45% v/v) microemulsion for topical delivery has been reported (Biruss et al. 2007). Results showed the ability of EO to augment percutaneous absorption by SC lipid extraction and loosening the hydrogen bond between the ceramides leading to fluidisation of lipid bilayers (Chen et al. 2014).

3.11 ***In vitro simulation***

Due to the ethical and financial burden imposed by *in vivo* studies, mathematical modelling or simulations studies are often used to predict dermal transport (Selzer et al. 2015). Simulations can aid to plan the *in vitro* experiments and understanding of the *in vitro* experiment results.

The applied model successfully predicted a drug distribution parameter (Kd Value) following transdermal application of TSN loaded formulation. The distribution parameter value (Kd) for the TSN formulation EO-6 is 0.001966 per cm^{-1} taking into consideration of the *in vitro* permeation data after 24 hours. Kd value is exceptionally low compared to similar kind of molecules like econazole (Schaefer and Stuttgen 1976). This would indicate the TSN is not systemically absorbed and that the formulation has potential for local targeting of the skin.

The formulation may have an impact on the Kd, once the Kd is known (also affected mostly by the physical properties of the drug), and then it is easier to calculate other parameters, which can be determined experimentally by several techniques (Zsiko et al. 2019). The model was further able to successfully characterize the relationship between observed topical exposure with *in vitro* drug permeation data after 24 hours and the intended pharmacological local dermal effect. % Cumulative triclosan

permeation through skin for drug formulation EO-6 at 24 hours is 1.38 µg/cm^2, which is also low and similar to the simulated Kd Value. Hence the predicted topical concentration of TSN based on simulations can be used to estimate the therapeutic effectiveness of a TSN for local dermal effect. (Schaefer and Zesch 1975; Gupta et al. 1995)

Commented [BC1]: Any discussion for this? Is there anything that can be taken from thisd https://openarchive.usn.no/usn-xmlui/handle/11250/2581937

Commented [MOU2]: I don't see anything that I can corelate with my results and discussion from the above paper..

4. Conclusion

In this study, essential oil based nanoemulsions were developed as a carrier for topical application of triclosan (TSN) to improve its skin permeability and to potentially yield synergistic therapeutic effects with respect to skin antisepsis. Nanoemulsions were prepared by high shear homogenization method with small droplet size and appreciable physical stability. Process and formulation variables were evaluated, and thermodynamic stability studies were carried out to identify thermodynamically stable and characterized formulation. In the present study, an optimized and thermodynamically stable TSN nanoemulsion was prepared using 5% w/w of S_{mix} and 5 and 10 % of essential oils. Our studies have clearly shown that TSN nanoemulsion was successfully formulated which was proved by pseudo-ternary phase diagrams and TEM studies. Studies confirm that triclosan is molecularly dispersed in essential oils with high encapsulation efficiency (78.80 to 86.14%) and formulations were stable. The average droplet size of prepared NEs decreased with increased homogenization time for both emulsions and the optimized homogenization time was 20 minutes. Furthermore, the *in vitro* permeation studies demonstrated that TSN nanoemulsions shows 3-4 times higher drug penetration into the skin from the EO-6 NE formulation compared to control solution. Modelling data indicated that NEs have good permeation as well as distribution throughout the dermis with limited potential for systemic absorption. This, the developed NEs may provide a local therapeutic effect, effectively

delivering TSN into the skin and hair follicles to prolong its antimicrobial activity. It is anticipated that the essential oils used in the nanoemulsion will also contribute to local antimicrobial activity. Hence, we can conclude that the process established in this study is an attractive option for nanoemulsion, as this technique leads to the production of stable and highly effective nanoemulsions of TSN for local dermal effect.

Acknowledgement

We would like to thank Dr. Jeremy Hopwood for TEM images and the University of Huddersfield for funding the project.

Disclosure of interest

The authors declare that they have no conflict of interest to report.

References

Aguiar J, Carpena P, Molina-Bolívar J, Carnero Ruiz C. 2003. On the determination of the critical micelle concentration by the pyrene 1:3 ratio method. J. Colloid Interface Sci. 258:116–122.

Ahmad N, Ahmad R, Al-Qudaihi A, Alaseel SE, Fita IZ, Khalid MS, Pottoo FH, Bolla SR. 2019. A novel self-nanoemulsifying drug delivery system for curcumin used in the treatment of wound healing and inflammation. 3 Biotech, 9(10):360.

Alvarado HL, Abrego G, Souto EB, Garduño-Ramirez ML, Clares B, García ML, Calpena AC. 2015. Nanoemulsions for dermal controlled release of oleanolic and ursolic acids: In vitro, ex vivo and in vivo characterisation. Colloids Surf B. 130:40-47.

Amin S, Kohli K, Khar RK, Mir SR, Pillai KK. 2008. Mechanism of in vitro percutaneous absorption enhancement of carvedilol by penetration enhancers. Pharm Dev Technol. 13:533-539.

Anissimov YG, Roberts MS. 2011. Modelling dermal drug distribution after topical application in human. Pharm Res. 28:2119-2129.

Azeem A, Rizwan M, Ahmad FJ, Iqbal Z, Khar RK, Aqil M, Talegaonkar S. 2009. Nanoemulsion components screening and selection: a technical note. AAPS PharmSciTech. 10(1):69-76.

Bali V, Ali M, Ali J. 2010. Study of surfactant combinations and development of a novel nanoemulsion for minimising variations in bioavailability of ezetimibe. Colloids Surf. B: Biointerfaces. 76:410–20.

Benita S, Levy MY. 1993. Submicron emulsions as colloidal drug carriers for intravenous administration: Comprehensive physicochemical characterisation. J Pharm Sci. 82:1069-1079.

Biruss B, K€ahlig H, Valenta C. 2007. Evaluation of an eucalyptus oil containing topical drug delivery system for selected steroid hormones. Int. J. Pharm. 328(2): 142–151.

Burt SA. 2004. Essential oils, their antibacterial properties and potential applications in foods: A review. Int J Food Microbiol. 94:223-253.

Cal K, Janicki S, Sznitowska M. 2001. In vitro studies on penetration of terpenes from matrix-type transdermal systems through human skin. Int. J. Pharm. 224(1-2):81–88.

Cal K, Kupiec K, Sznitowska M. 2006. Effect of physicochemical properties of cyclic terpenes on their ex vivo skin absorption and elimination kinetics. J. Dermatol. Sci. 41(2):137–142.

Cao Z, Spilker T, Fan Y, Kalikin LM, Ciotti S, LiPuma JJ, Makidon PE, Wilkinson JE, Baker JR Jr, Wang SH. 2017. Nanoemulsion is an effective antimicrobial for methicillin-resistant Staphylococcus aureus in infected wounds. Nanomedicine (Lond). 12(10):1177-1185.

Charkoudian N. 2003. Skin blood flow in adult human thermoregulation: How it works, when it does not, and why. Mayo Clinic Proceedings, May 78(5):603-612.

Chanamai R, McClements DJ. 2000. Dependence of creaming and rheology ofmonodisperse oil-in-water emulsions on droplet size and concentration. Colloids Surf A Physicochem. 172:79-86.

Chen H, Chang X, Weng T, Zhao X, Gao Z, Yang Y, Xu H, Yang X. 2004. A study of microemulsion systems for transdermal delivery of triptolide. J Control Release. 98(3):427-36.

Chen Y, Quan P, Liu X, Wang M, Fang L. 2014. Novel chemical permeation enhancers for transdermal drug delivery. Asian J. Pharm. Sci. 9(2):51–64.

Chiesa M, Garg J, Kang YT, Chen G. 2008. Thermal conductivity and viscosity of water-in-oil nanoemulsions. Colloids Surf A Physicochem. 326:67-72.

Cooper R, Kirketerp-Møller K. 2018. Non-antibiotic antimicrobial interventions and antimicrobial stewardship in wound care. J Wound Care. 27 (6):355-377.

Cornwell PA, Barry BW, Bouwstra JA, Gooris GS. 1996. Modes of action of terpene penetration enhancers in human skin: differential scanning calorimetry, small-angle X-ray diffraction and enhancer uptake studies. Int. J. Pharm. 127(1):9–26.

Chou TH, Nugroho DS, Chang JY, Cheng YS, Liang CH, Deng MJ, 2021. Encapsulation and Characterization of Nanoemulsions Based on an Anti-oxidative Polymeric Amphiphile for Topical Apigenin Delivery. Polymers. 13:1016.

Cross SE, Roberts MS. 2006. Dermal blood flow, lymphatics, and binding as determinates of topical absorption, clearance, and distribution. In: Riviere JE, editor. Dermal absorption models and pharmacology. Boca Raton: CRC Press; p. 251-282.

Demisli S, Mitsou E, Pletsa V, Xenakis A, Papadimitriou V. 2020. Development and Study of Nanoemulsions and Nanoemulsion-Based Hydrogels for the Encapsulation of Lipophilic Compounds. Nanomaterials (Basel). 10(12):2464.

Dominik S, Dirk N, Ulrich F. 2015. Mathematical models for dermal drug absorption. Expert Opin Drug Metab Toxicol. 11(10):1-17.

Elisabet F, Clara R, Martí R, Elisabeth B. 2005. Critical micelle concentration of surfactants in aqueous buffered and unbuffered systems. Anal. Chim. Acta. 548:95–100.

Ghiasia Z, Esmaelia F, Aghajania M, Ghazi M, Mohammad K, Faramarzic A. 2019. Enhancing analgesic and anti-inflammatory effects of capsaicin when loaded into olive oil nanoemulsion: An in vivo study. Int J Pharm. 559:341-347.

Grosse C, Pedrosa S, Shilov VN. 2002. On the influence of size, zeta potential, and state of motion of dispersed particles on the conductivity of a colloidal suspension. J Colloid Interface Sci. 251:304-310.

Gupta E, Wientjes MG, Au JL. 1995. Penetration kinetics of 2′,3′- dideoxyinosine in dermis is described by the distributed model. Pharm Res. 12:108-112.

Hemmila MR, Mattar A, Taddonio MA, Arbabi S, Hamouda T, Ward PA, Wang SC, Baker JR Jr. 2010. Topical nanoemulsion therapy reduces bacterial wound infection and inflammation after burn injury. Surgery. 148(3):499-509.

Herman A, Andrzej P. 2015. Essential oils and their constituents as skin penetration enhancer for transdermal drug delivery: a review. J Pharm Pharmacol. 67(4):473-485.

Heuschkel S, Goebel A, Neubert RHH. 2008. Microemulsions-morden colloidal carrier for dermal and transdermal drug delivery. J Pharm Sci. 97:603-631.

Hilton J, Woollen BH, Scott RC, Auton TR, Trebilcock KL, Wilks MF. 1994. Vehicle effects on in vitro percutaneous absorption through rat and human skin. Pharm. Res. 11:1396–1400.

Kakadia PG, Conway BR. 2018. Solid lipid nanoparticles for targeted delivery of triclosan into skin for infection prevention. J Microencapsul. 35:695-704.

Karpanen TJ, Conway BR, Worthington T, Hilton AC, Elliott TS, Lambert PA. 2010. Enhanced chlorhexidine skin penetration with eucalyptus oil. BMC Infect Dis. 10:278.

Kaseem MGA, Ahmed AMM, Abdel-Rehman HH, Moustafa AHE. 2019. Use of Span 80 and Tween 80 for blending gasoline and alcohol in spark ignition engines. Energy Rep. 5:221-230.

Kuo SH, Shen CJ, Shen CF, Cheng CM, 2020. Role of pH value in clinically relevant diagnosis. Diagnostics. 10(107):1-17.

Lademann J, Jacobi U, Surber C, Weigmann HJ, Fluhr JW. 2009. The tape stripping procedure - Evaluation of some critical parameters. Eur J Pharm Biopharm. 72:317-323.

Lan Y, Wu Q, Mao YQ, Wang Q, An J, Chen YY, Wang WP, Zhao BC, Liu N, Zhang YW. 2014. Cytotoxicity and enhancement activity of essential oil from Zanthoxylum bungeanum Maxim. as a natural transdermal penetration enhancer. J Zhejiang Univ Sci B. 15(2):153-64.

Lange-Asschenfeldt B, Marenbach D, Lang C, Patzelt A, Ulrich M, Maltusch A, Terhorst D, Stockfleth E, Sterry W, Lademann J. 2011. Distribution of bacteria in the epidermal layers and hair follicles of the human skin. Skin Pharmacol Physiol. 24(6):305-311.

Laouini A, Jaafar-Maalej C, Limayem-Blouza I, Sfar S, Charcosset C, Fessi H. 2012. Preparation, characterization, and applications of liposomes: state of the art. J Colloid Sci Biotechnol. 1:147-168.

Lawrence MJ, Rees GD. 2000. Microemulsion-based media as novel drug delivery systems. Adv Drug Deliv Rev. 45:89-121.

Lee PJ, Langer R, Shastri VP. 2003. Novel microemulsion enhancer formulation for simultaneous transdermal delivery of hydrophilic and hydrophobic drugs. Pharm. Res. 20:264–269.

Loo CH, Basri M, Tejo BA, Ismail R, Nang HLL, Hassan HA, Choo YM. 2011. An improved method for the preparations of nanostructured lipid carrierr containing heat-sensitive bioactives. Colloids Surf B. 87:180-186.

Maillard V. 2013. Factors affecting the activities of microbicides. In: Russell, Hugo & Ayliffe's Principles and Practice of Disinfection, Preservation and Sterilization (5th edn). Fraise A.P., Maillard, J-Y. Satter, S.A. (eds). Wiley-Blackwell.

Malcolmson C, Satra C, Kantaria S, Sidhu A, Lawrence MJ. 1998. Effect of oil on the level of solubilization of testosterone propionate into nonionic oil-in-water microemulsions. J Pharm Sci. 87:109-116.

Mayer S, Weiss J, McClements DJ. 2013. Behavior of vitamin E acetate delivery systems under simulated gastrointestinal conditions: Lipid digestion and

bioaccessibility of low energy nanoemulsions. J Colloid Interface Sci. 404:215-222.

McClements DJ, Xiao H. 2012. Potential biological fate of ingested nanoemulsions: Influence of particle characteristics. Food Func. 3:202-220.

Moghimipoura E, Salimi A, Jahromic A. 2018. Influence of chemical permeation enhancers on the in vitro skin permeation of minoxidil through excised rat skin: a mechanistic study. Iran J Pharm Sci. 14(1):97-110.

Nastiti CMRR, Ponto T, Mohammed Y, Roberts MS, Benson HAE. 2020. Novel Nanocarriers for Targeted Topical Skin Delivery of the Antioxidant Resveratrol. Pharmaceutics. 12(2):108.

O'Neil MJ. (ed.)2013. The Merck Index An Encyclopedia of Chemicals, Drugs, andBi ologicals. Cambridge, UK: Royal Society of Chemistry, p. 1789.

Prasad, C., Bhatia, E., Banerjee, R. 2020. Curcumin Encapsulated Lecithin Nanoemulsions: An Oral Platform for Ultrasound Mediated Spatiotemporal Delivery of Curcumin to the Tumor. Sci Rep. 10:8587.

Quiñones OG, Hossy BH, Padua TA, Miguel NCO, Rosas EC, Ramos MFS, Pierre MBR. 2018. Copaiba oil enhances in vitro/in vivo cutaneous permeability and in vivo anti-inflammatory effect of celecoxib. J Pharm Pharmacol. 70(7):964-975.

Salager JL, Anderez JM, Briceno MI, Sánchez MP, Gouveia MR. 2002. Emulsification yield related to formulation and composition variables as well as stirring energy. Revista Tecnica de la Facultad de Ingenieria Universidad del Zulia. 25:129-139.

Saporito F, Sandri G, Bonferoni MC, Rossi S, Boselli C, Icaro Cornaglia A, Mannucci B, Grisoli P, Vigani B, Ferrari F. 2018. Essential oil-loaded lipid nanoparticles for wound healing. Int. J. Nanomedicine. 13:175–186.

Schaefer H, Stuttgen G. 1976. Absolute concentrations of an antimycotic agent, econazole, in the human skin after local application. Arzneimittelforschung. 26(3):432-435.

Schaefer H, Zesch A. 1975. Penetration of vitamin A acid into human skin. Acta Derm Venereol Suppl (Stockh). 74:50-55.

Selzer D, Neumann D, Neumann H, Kostka K-H, Lehr C-M, Schaefer UF. 2015. A Strategy for In-Silico Prediction of Skin Absorption in Man. Eur J Pharm Biopharm. 95:68-76.

Shahavi MH, Hosseini M, Jahanshahi M, Meyer RL, Darzi GN. 2015. Evaluation of critical parameters for preparation of stable clove oil nanoemulsion. Arab J Chem. 12:3225-3230.

Shen T, Xu H, Weng W, Zhang J. 2013. Development of a reservoir-type transdermal delivery system containing eucalyptus oil for tetramethylpyrazine. Drug Deliv. 20:19-

Srilatha R, Aparna C, Srinivas P, Sadananda M. 2013. Formulation, evaluation and characterisation of glipizide nanoemulsion. Asian J Pharm Clin Res. 6:66-71.

Sugumar S, Ghosh NM, Mukherjee A, Chandrasekaran N. 2014. Ultrasonic emulsification of eucalyptus oil nanoemulsion: Antibacterial activity against *Staphylococcus aureus* and wound healing activity in Wistar rats. Ultrason Sonochemistry. 21(3):1044-1049.

Tagne JB, Kakurnanu S, Nicolosi RJ. 2008. Nanoemulsion preparations of the anticancer drug dacarbazine significantly increase its efficacy in a xenograft mouse melanoma model. Mol Pharm. 5:1055-1063.

Teichmann A, Jacobi U, Ossadnik M, Richter H, Koch S, Sterry W, Lademann J. 2005. Differential stripping: Determination of the amount of topically applied substances penetrated into the hair follicles. J Investig Dermatol. 125:264-269.

Tripathy M. 2014. Comparison of process parameter optimisation using different designs in nanoemulsion based formulation for transdermal delivery of fullerene. Int J Nanomedicine. 9:4375-4386.

Vatsraj S, Chauhan K, Pathak H. 2014. Formulation of a novel nanoemulsion system for enhanced solubility of a sparingly water soluble antibiotic, clarithromycin. J Nanosci. 1-7.

Weigmann HJ, Schanzer S, Patzelt A, Bahaban V, Durat F, Sterry W, Lademann J. 2009. Comparison of human and porcine skin for characterisation of sunscreens. J Biomed Opt. 14:24-27.

Wilke CR, Chang P. 1955. Correlation of diffusion coefficients in dilute solutions. AIchE J. 1(2):264-270.

Williams AC, Barry BW. 1989. Essential oils as novel human skin penetration enhancers. Int J Pharm. 57:7-9.

Williams AC, Edwards HGM, Lawson EE, Barry BW. 2006. Molecular interactions between the penetration enhancer 1,8-cineole and human skin. J. Raman Spectrosc. 37(1–3):361–366.

Wooster TJ. 2008. Impact of oil type on nanoemulsion formation and Ostwald ripening stability. Langmuir. 24:12758-12765.

Wosika H, Cal K. 2010. Targeting to hair follicles: Current status and potential. J Dermatol Sci. 57:83-89.

Yu M, Ma H, Lei M, Li N, Tan F. 2014. In vitro/in vivo characterization of nanoemulsion formulation of metronidazole with improved skin targeting and anti-rosacea properties. Eur J Pharm Biopharm. 88:92-103.

Zsikó S, Csányi S, Kovács A, Budai M, Gácsi A, Berkó S. 2019. Methods to evaluate

skin penetration in vitro. Sci Pharm. 87:19.

Table Captions

Table 1: Parameters considered for *in vivo* simulation studies of TSN-loaded NE (Eucalypts oil Nanoemulsion 6)

Table 2: Solubility of TSN obtained after 48 h equilibration at 25°C (mean ± SD, n = 3).

Table 3: Physicochemical characterisation of optimised NEs formulations (Mean ± SD, n = 3).

Table 4: Composition and observation for thermodynamic stability study and dispersibility test of TSN-loaded NE formulations.

Table 5. In vitro permeability parameters of TSN-loaded NE formulations and control solution in porcine ear skin (Mean ± SD, n = 6).

Table 1

Variable	Parameter	Value
In vitro permeation data	Porcine ear skin thickness	500 µm
	pH	7.4
	The amount of TSN from formulation EO6	
	permeated through skin over 24 h.	1.38 µg/cm^2
	Partition coefficient of TSN	4.7
API/Formulation data	pKa or ionization status of TSN at skin pH	7.9
	(O'Neil 2013)	
	Dosage of TSN	10 mg/ml
	Surface area for skin application	3.8 cm^2
In vivo data	Blood flow	250 ml /min
	(**Charkoudian 2003)**	

Table 2

Medium	Solubility (mg/g)
Control Solution	10.05 ± 0.24
EO	5.23 ± 0.02
OO	3.51 ± 0.05
T80	41.23 ± 0.08
S80	29.13 ± 0.03

Table 3

Formulation Code	ZP (mV)	% EE	pH	Viscosity (cP)

EO-2	-37.1 ± 1.72	78.83 ± 1.28	5.23	20.08 ± 1.14
EO-6	-31.8 ± 0.91	86.14 ± 0.93	5.71	24.15 ± 0.94
OO-2	-34.5 ± 1.21	75.49 ± 1.16	5.54	22.31 ± 1.29
OO-6	-28.9 ± 1.23	81.19 ± 2.15	5.91	28.46 ± 1.73

Table 4

Formulation	**%S_{mix}**	**%Oil**	**%Water**	**H/C[a]**	**Centr.[b]**	**F/T[c]**
EO-1	2.5	5	92.5	X	-	-
EO-2	5	5	90	√	√	√
EO-3	10	5	85	√	X	-
EO-4	2.5	10	92.5	X	-	-
EO-5	5	10	90	√	√	√
EO-6	10	10	85	X	-	-
OO-1	2.5	5	92.5	√	X	-
OO-2	5	5	90	√	√	√
OO-3	10	5	85	√	X	-
OO-4	2.5	10	92.5	√	X	-
OO-5	5	10	90	√	√	√
OO-6	10	10	85	X	-	-

a = Heating-cooling cycle. b = Centrifugation. C = Freeze-thaw cycle.
√ = stable (no phase separation), X = unstable (phase separation), N/A = (not applicable)

Table 5

Formulation	**Flux (J_{ss}) µg/cm^2/h**	**Permeability coefficient (K_p) x 10^{-5} cm/h**
Control	0.074 ± 0.07	0.91 ± 0.13

OO-2	0.302 ± 0.07	2.73 ± 0.06
OO-6	0.385 ± 0.03	3.15 ± 0.12
EO-2	0.479 ± 0.04	3.79 ± 0.16
EO-6	0.638 ± 0.06	5.06 ± 0.38

Figure Captions

Figure 1: Pseudoternary phase diagrams of A. (a) Eucalyptus oil (EO) (b-e) combinations containing EO, water and surfactant mixture at Smix (T80:S80) ratios of 1:1, 2:1, 3:1, and 4:1 respectively. B. a) Olive oil (OO) (b-e) combinations containing OO, water and surfactant mixture at Smix (T80:S80) ratios of 1:1, 2:1, 3:1 and 4:1 respectively.

Figure 2: Impact of homogenization on EO-NE and OO-NE droplet size (Mean ± SD, n = 3).

Figure 3: TEM image of TSN-loaded NEs (EO-5;5).

Figure 4: *In vitro* skin permeation profile of NE formulations (EO-2, EO-6, OO-2, OO-6) and control (Mean ± SD, n = 6).

Figure 5: *In vitro* profile of TSN accumulation in skin layers 24 h following topical application of control, the EO-NEs (EO-2, EO-6), and the OO-NEs (OO-2, OO-6). (Mean ± SD, n = 6). HOMO refers to homogenised tissue after removal of the SC layers.

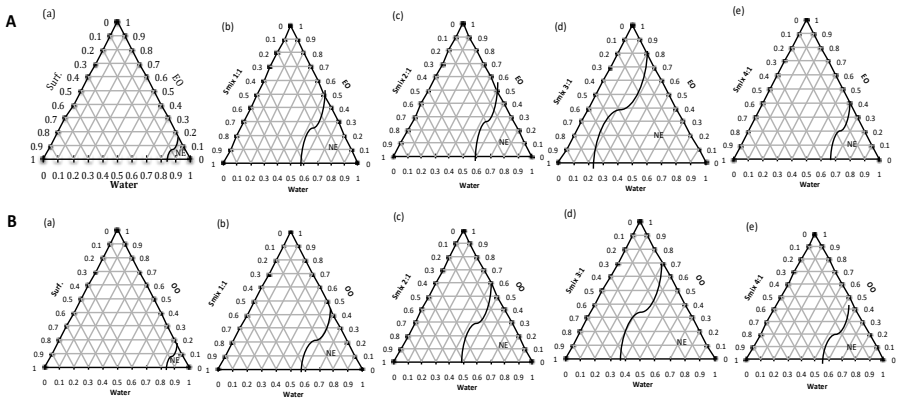
A
(a)
(b)
(c)
(d)
(e)
Surf.
Smix 1:1
Smix 2:1
Smix 3:1
Smix 4:1
OD
NE
Water
B
(a)
(b)
(c)
(d)
(e)
Surf.
Smix 1:1
Smix 2:1
Smix 3:1
Smix 4:1
OD
NE
Water

Figure 1

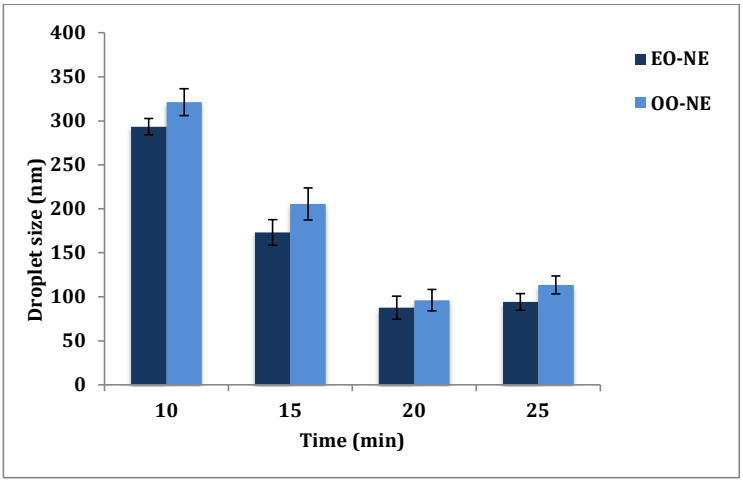

Figure 2

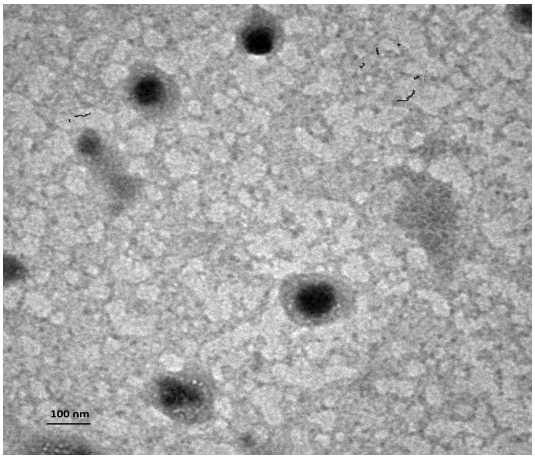

Figure 3

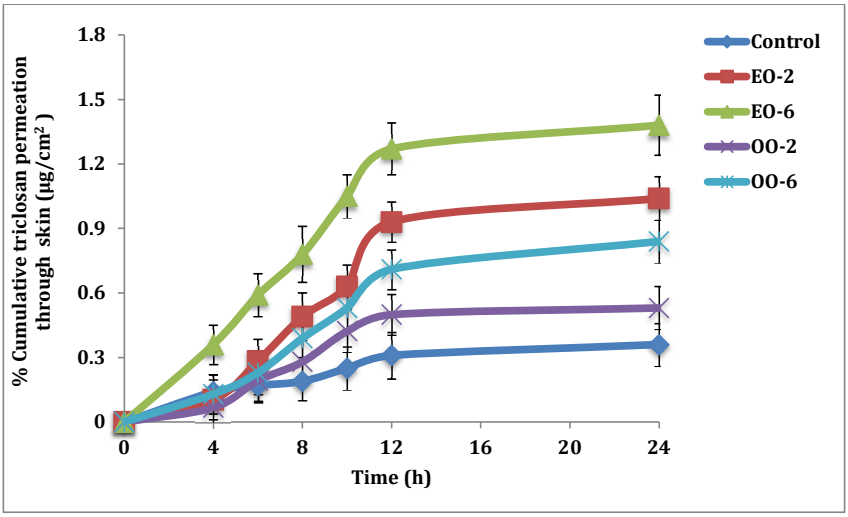

Figure 4

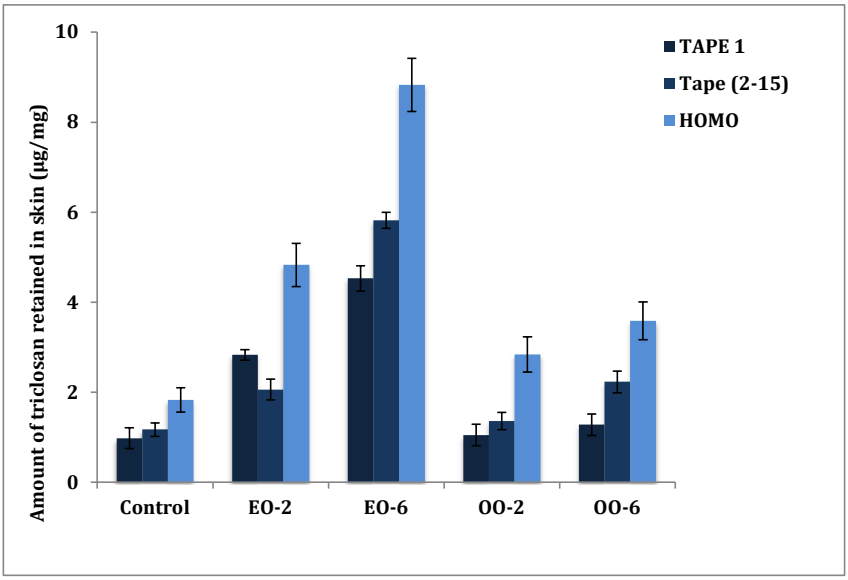

Figure 5